

Heat and Mass Transfer Past a Semi- Infinite Vertical Porous Plate in MHD Flows in Turbulent Boundary Layer

Ngesa Joel Ochola, Kennedy Otieno Awuor, Jeconia Okello Abonyo, Mark Erick M. Kimathi

Abstract- This study addresses the problem of unsteady free convection incompressible MHD fluid flow past a semi-infinite vertical porous plate in the presence of a strong magnetic field inclined at an angle θ to the plate with Hall and Ion-Slip currents. It investigates the effects of Grashof number, heat source parameter, suction velocity, time, angle of inclination, Ion-Slip, Hall current and mass diffusion parameter on the convectively cooled or convectively heated plate restricted to turbulent boundary layer of the flow field. The partial differential equations governing the flow problem considered in our study are solved by a finite difference approximation while the computation of skin friction, rate of heat transfer and mass transfer at the plate is achieved by Newton's interpolation approximation over the first five points. The results show that the Hall current, Schmidt number, Modified Grashof number, heat source parameter, suction velocity, time, angle of inclination, Ion-Slip current on the convectively cooled or convectively heated plate affect the velocity, temperature and concentration profiles. Increases in Hall parameter cause a decrease in both primary and secondary profiles while increase in Ion Slip current parameter leads to increase in primary velocity profiles but a decrease in secondary velocity profiles. Consequently, their effects alter the skin friction, rate of mass transfer and the rate of heat transfer.

Index Terms- Heat transfer, Mass transfer, MHD, Turbulent flow, Semi-infinite plate, Hall and Ion-Slip currents.

I. INTRODUCTION

A. Convection Heat Transfer

Convection heat transfer involves the energy exchange between a boundary surface and the adjacent fluid due to temperature variations. It's not possible to separate the problem of heat transfer from that of the motion of the fluid, and so a study of the hydrodynamic behaviour of the fluid is very much necessary in order to gain an understanding of the heat transfer phenomena within a moving fluid. Analysis of this behaviour requires the application of the principles of conservation of mass (continuity equation), Newton's laws of motion (momentum equations), and the laws of thermodynamics (energy equation) along with the phenomenological laws like Fourier's laws, Fick's laws and Newton's law of viscosity.

Ngesa Joel Ochola Machakos University
Kennedy Otieno Awuor Kenyatta University
Jeconia Okello Abonyo Jomo Kenyatta University of Agriculture and Technology
Mark Erick M. Kimathi, Machakos University

Fluids include both liquids and gases. While liquids are incompressible, gases are compressible, having their densities varying with pressure greatly, and also with temperature.

The study of heat transfer by convection is concerned with the calculation of rates of heat exchange between fluids and solid boundaries. Transfer of fluids between solids and fluid involves the mass, momentum and heat transfer. Modes of heat transfer are by conduction, convection and radiation.

B. Mass Transfer

The bulk flow of fluid due to pressure gradient occurring at a macroscopic level is a kind of mass transfer usually treated in the subject of fluid mechanics. In this work our concern is mass transfer occurring at a microscopic or molecular level, which deals with the transport of one constituent of a fluid solution or gas mixture from a region of higher concentration to a region of lower concentration. Heat is transferred in a direction which reduces an existing temperature gradient, and mass is transferred in a direction which reduces an existing concentration gradient. Drying, evaporation, chemical reaction, absorption, adsorption, solution and so on are all instances of mass transfer.

C. Magnetohydrodynamics (MHD)

MHD studies the motion of electrically conducting fluid in the presence of a magnetic field. This motion leads to induced electric currents on which mechanical forces are exerted by magnetic field. The induced electric currents in turn produce induced magnetic field which affect the original magnetic field.

D. Hall And Ion-Slip Currents

The electrical current density \vec{J} represents the relative motion of charged particles in a fluid. The equation of electric current density may be derived from the diffusion velocities of the charged particles. The major forces on charged particles are electromagnetic forces. If we consider only the electromagnetic forces, we may obtain the generalized Ohm's law. However, the deduction from the diffusion velocity of charged particles is more complicated

than the generalized Ohm's law. When electric field \vec{E} is applied, there will be an electric current in the direction of \vec{E} . If the magnetic field \vec{H} is perpendicular to \vec{E} , there will be an electromagnetic force $\vec{J} \times \vec{B}$, which is perpendicular to both \vec{E} and \vec{H} , which is known as Hall

current. For the same electromagnetic force, the motion of ions is different from that of electrons, when the electromagnetic force is very large (such as in a very strong magnetic field) the diffusion velocity of ions cannot be neglected. If we consider the diffusion velocity of ions as well as that of electrons, we have the phenomenon of Ion-slip current.

In turbulent flow, the transport mechanism is aided by innumerable eddies. Irregular velocity fluctuations are superimposed upon the motion of the main stream, and these fluctuations are primarily responsible for the transfer of heat as well as momentum.

The fluid motion may be caused by external mechanical means for example by a fan, pumps, in which case the process is called forced convection. If the fluid motion is caused by density differences which are created by the temperature differences existing in the fluid mass, the process is called free convection or natural convection. In natural convection, flow velocities are produced by the buoyancy forces only; hence there are no externally induced flow velocities. As a result, the Nusselt number doesn't depend on Reynolds number.

Buoyant force causes denser parts of the fluid to move downwards and less dense parts to move upwards. The density differences can result from various effects such as differences in concentration of dissolved matter or in temperature.

Typical examples of turbulent flows are flow around, as well as in cars, Aeroplanes and buildings.

II. LITERATURE REVIEW

Yamamoto and Tomoaki (2011) discussed heat transfer degradation in high Prandtl number fluid which was evaluated via direct numerical simulation (DNS). Target flow fields were fully developed turbulent channel flows imposed a wall-normal magnetic field in the high and low Prandtl number conditions ($Pr = 5.25$ and 0.025 , respectively). Values of the bulk Reynolds number ($Re_b = 14,000$) and the Hartmann number

($Ha = 0-32$) were set to be equivalent to those of the previous experimental study by Yokomine et al. The numerical results of the Nusselt number for the high Prandtl number fluid were in good agreement with the experimental results.

Xenos M. et al. (2009), researched on methods of optimizing separation of compressible turbulent boundary-layer flow over a wedge with heat and mass transfer, the steady, compressible, turbulent boundary-layer flow, with heat and mass transfer, over a wedge, is numerically studied. The obtained results show that the flow field can be controlled by the suction/injection velocity and it is influenced by the dimensionless pressure parameter m .

Shin-ichi et al (2010) studied direct numerical simulation of unstable stratified turbulent flow under a magnetic field, in this research; liquid-metals as coolant material in a fusion reactor have a significant role in the design of advanced

reactors. Using the simulation, they observed that with an increase in heat transfer, thermal plume by the effect of buoyancy filled the entire region of the channel. In case of an applied magnetic field, it was seen that the turbulence became weak with the magnetic field, although the thermal transport was also increased by the buoyancy effect of the thermal plume.

Mathew Kinyanjui et al. (2012) investigated a turbulent flow of a rotating system past a semi-infinite vertical porous plate. They considered the flow in the presence of a variable magnetic field. They noted that the Hall current, rotation, Eckert number, injection and Schmidt number affect the velocity, temperature and concentration profiles.

Bo Lu et al. (2013) did a study on three dimensional MHD simulation of the electromagnetic flow meter for laminar and turbulent flows, their Numerical results show that induced electric potential difference at the electrodes agreed with the theoretical values. Simulations also render the detailed distributions of induced electric field, current density, electric potential and induced magnetic field. Buffetta G. et al. (2012) in their paper, the ultimate state of thermal convection in Reyleigh-Taylor turbulence, discusses the so-called ultimate state of thermal convection, first proposed by Kraichnan almost 50 years ago and recently observed in numerical simulations of turbulent convection in the absence of boundaries. They focus on numerical simulations of turbulence generated by the Rayleigh-Taylor instability in a wide range of Rayleigh and Prandtl numbers and results point out to the conclusion that RT turbulence provides a natural realization of the ultimate state of thermal convection thus highlighting the relationship between the absence of boundaries and the emergence of the ultimate state scaling for global statistical quantities.

Sanvincente E et al. (2013) had an experimental study on natural convection flows in a differentially heated open channel configuration. The applications concern the free cooling of both the photovoltaic components integrated within the building envelope (double-skin configuration) and the building itself. Particular focus is given to the identification of integration configurations favorable to both heat transfer on the rear side of components and buoyancy enhancement. The test section consists of a vertical channel with two walls composed of different heating modules. In the present investigation the thermal configuration considers one wall heated uniformly while the other is not heated. They focus on the kinematic characteristics of the flow and convective heat transfer at the heated wall. The experimental evidence shows that the flow is neither really turbulent nor purely laminar for the range of Rayleigh numbers considered. Although the average characteristics of the flow seem perfectly consistent with the results obtained, changes of behavior seem to occur intermittently.

Mohammad ZoynalAbedin et al. (2012) carried out study on turbulence characteristics and vertical structures in combined convection boundary layers along a heated vertical flat plate, They performed Time-developing direct numerical simulations for the combined-convection

boundary layers created by imposing aiding and opposing free streams to the pure natural-convection boundary layer in air along a heated vertical flat plate to clarify their structural characteristics. The numerical results reveal that with a slight increase in free stream velocity, the transition region moves downstream for aiding flow and upstream for opposing flow. Mathew Kinyanjui et al. (2012) investigated a turbulent flow of a rotating system past a semi-infinite vertical porous plate. They considered the flow in the presence of a variable magnetic field. They noted that the Hall current, rotation, Eckert number, injection and Schmidt number affect the velocity, temperature and concentration profiles.

Yasuo Hattori et al. (2006) did investigate on the turbulence characteristics of a natural-convection boundary layer in air along a vertical plate heated at high temperatures experimentally. In their study two-dimensional velocity vectors and instantaneous temperature in the boundary layer at a wall temperature up to 300 °C are measured using a particle image velocimetry and a cold wire found that heat transfer rates even for a wall temperature of 300 °C are well expressed by an empirical formula obtained for low wall temperature and the region of transition from laminar to turbulence does not change much with an increase in wall temperature. In addition, the profiles of turbulent quantities measured at a wall temperature of 300 °C resemble those observed at low wall temperatures, and thus the effects of high heat on the turbulent behavior in the boundary layer are quite small. The measured velocity vectors and the higher-order statistics, such as skewness and flatness factors of fluctuating velocities and temperature, also suggest that the structure of large-scale fluid motions in the outer layer of the natural-convection boundary layer, closely connected with turbulence generation, is maintained even under high wall temperature conditions.

III. SPECIFIC EQUATIONS GOVERNING FLUID FLOW

The equations governing incompressible unsteady free convection fluid flow in the presence of heat and mass transfers are considered. In this study unsteady free convection magnetohydrodynamic flow past a semi-infinite vertical porous plate subjected to a strong magnetic field inclined at an angle of θ to the plate and constant suction is studied. The x^* -axis is taken along the plate in vertically upward direction, which is the direction of flow.

The z^* -axis taken normal to the plate, since the plate is semi-infinite in length and for a two-dimensional free convective fluid flow the physical variables are functions of x^* , z^* and t^* . The fluid is permeated by a strong magnetic field $\vec{H} = (H_0 \sqrt{1-\psi^2}, 0, H_0 \psi)$ where $H_0 = |H|$ is the magnitude of the magnetic field and $\psi = \cos\theta$.

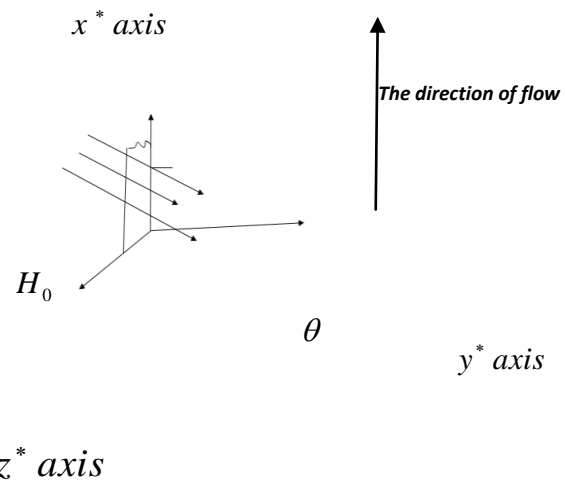


Figure 1: showing flow configuration
 The continuity equation for the fluid flow under consideration is given by;

$$\frac{\partial w^*}{\partial z^*} = 0 \quad (1)$$

Since the fluids particle velocity equal to zero because of no-slip condition. On integration equation (3.4.9) gives the constant suction velocity

$$w^* = -w_0^* \quad (2)$$

To determine the pressure gradient term in momentum equation

$$\rho \left(\frac{\partial U_j}{\partial t} + U_j \frac{\partial U_i}{\partial x_j} \right) = -\frac{\partial p}{\partial x_j} + \rho \nu \nabla^2 U_i + \rho g + J \times B$$

the momentum equation is evaluated at the edge of the boundary layer where $\rho \rightarrow \rho_\infty$ and $U \rightarrow 0$. The

pressure term in the x^* direction, $-\frac{\partial p}{\partial x^*} = -\rho_\infty g$ results from the change in the elevation. The body force term in eqn. 2.7 along negative x^* direction is $-\rho g$. Combining the pressure term and the body force term gives.

$$-\rho g - \frac{\partial p}{\partial x^*} = g(\rho_\infty - \rho) \quad (3)$$

If the volumetric coefficient of thermal expansion is defined by

$$\beta = -\frac{1}{\rho} \left(\frac{\Delta \rho}{\Delta T} \right)_p = -\frac{1}{\rho} \left(\frac{\rho_\infty^* - \rho^*}{T_\infty^* - T^*} \right) = \frac{1}{\rho} \left(\frac{\rho_\infty^* - \rho^*}{T^* - T_\infty^*} \right) \quad (4)$$

and the volumetric coefficient of thermal expansion with concentration of the fluid by

$$\beta' = -\frac{1}{\rho} \left(\frac{\Delta \rho}{\Delta C} \right)_p = -\frac{1}{\rho} \left(\frac{\rho_\infty^* - \rho^*}{C_\infty^* - C^*} \right) = \frac{1}{\rho} \left(\frac{\rho_\infty^* - \rho^*}{C^* - C_\infty^*} \right) \quad (5)$$

From equation (1) and equation (2) we have,

$$\beta\rho(T^* - T_\infty^*) = p_\infty^* - p^* \quad (6)$$

$$\beta'\rho(C^* - C_\infty^*) = p_\infty^* - p^*$$

The total change in density as a result of temperature and concentration is given by

$$\Delta\rho = \beta\rho(T^* - T_\infty^*) + \beta'\rho(C^* - C_\infty^*)$$

From Ohm's law $J = \sigma(q \times B)$, where J is the electric current density $J = (J_{x^*}, J_{y^*}, J_{z^*})$ and B is the magnetic induction, $B = (\mu_e H)$ which in component form is given as,

$$B_{x^*} = \mu_e H_0 \sin \theta$$

$$B_{y^*} = 0$$

$$B_{z^*} = \mu_e H_0 \cos \theta$$

$$J = \sigma \begin{vmatrix} i & j & k \\ u^* & v^* & 0 \\ B_{x^*} & 0 & B_{z^*} \end{vmatrix} = \sigma(v^* B_{z^*} i - u^* B_{z^*} j) = \sigma \mu_e H_0 \psi (v^* i - u^* j) \quad (8)$$

Where the term in equation (2.7) can be simplified as,

$$J \times B = \begin{vmatrix} i & j & k \\ J_{x^*} & J_{y^*} & 0 \\ \mu_e H_0 \sqrt{1-\psi^2} & 0 & \mu_e H_0 \psi \end{vmatrix} = i J_{y^*} \mu_e H_0 \psi - j J_{x^*} \mu_e H_0 \quad (9)$$

From the equation of conservation of electric charges $\nabla \cdot J = 0$, gives $J_{z^*} = \text{constant}$, this constant is zero, since $J_{z^*} = 0$ at the plate which is electrically non-conducting hence $J_{z^*} = 0$ everywhere in the flow, $B_{y^*} = 0$ due to the geometrical nature of our problem.

Substituting equations (3.5.5) and (3.5.7) in equation (3.4.2) and writing the result in component form to obtain;

$$\rho \left(\frac{\partial u^*}{\partial t^*} + u^* \frac{\partial u^*}{\partial x^*} - w_0^* \frac{\partial u^*}{\partial z^*} \right) = \mu \left(\frac{\partial^2 u^*}{\partial x^{*2}} + \frac{\partial^2 u^*}{\partial z^{*2}} \right) + \beta\rho(T^* - T_\infty^*) + \beta'\rho(C^* - C_\infty^*) + \mu_e \psi H_0 J_{x^*} \quad (10)$$

$$\rho \left(\frac{\partial v^*}{\partial t^*} + u^* \frac{\partial v^*}{\partial x^*} - w_0^* \frac{\partial v^*}{\partial z^*} \right) = \mu \left(\frac{\partial^2 v^*}{\partial x^{*2}} + \frac{\partial^2 v^*}{\partial z^{*2}} \right) - \mu_e \psi H_0 J_{y^*} \quad (11)$$

The generalized ohm's law including the effect of Hall current is written as;

$$j + \frac{we\tau e}{H} (j \times H) = \delta \left[E + \mu_e (q \times H) + \frac{1}{e\eta_e} \nabla p_e \right] \quad (12)$$

For the partially ionized fluids the electron pressure gradient may be neglected.

In this case we consider a short circuit problem in which the applied electronic field =0. Thus neglecting electron pressure the x and y components become;

$$j + \frac{we\tau e}{H} (j \times H) = \delta \mu_e (q \times H) \quad (13)$$

Expanding the equation we get

$$(J_{y^*}, J_{z^*}) + \frac{we\tau e}{H} (j_z H_0, -j_y H_0) = \delta \mu_e (v H_0 - w_0 H_0) \quad (14)$$

Solving these equations for current density components j_y and j_z

$$J_{y^*} = \frac{\delta \mu_e H_0 (mv - w)}{1 + m^2} \quad (7)$$

$$J_{z^*} = -\frac{\delta \mu_e H_0 (v - mw)}{1 + m^2} \quad (16)$$

Where $m = we\tau$ is the hall parameter.

Substituting equations (3.48) and (3.49) in the momentum equations and introducing the shear stress terms $\frac{\partial uv}{\partial x}$ and

$$\frac{\partial uw}{\partial x} \text{ yields}$$

$$\rho \left(\frac{\partial u^*}{\partial t^*} + u^* \frac{\partial u^*}{\partial x^*} - w_0^* \frac{\partial u^*}{\partial z^*} \right) = \mu \left(\frac{\partial^2 u^*}{\partial x^{*2}} + \frac{\partial^2 u^*}{\partial z^{*2}} \right) + \beta\rho(T^* - T_\infty^*) + \beta'\rho(C^* - C_\infty^*) - \frac{\partial uv}{\partial x} + \frac{\delta \psi \mu_e^2 H_0^2 (mv - w)}{1 + m^2} \quad (17)$$

$$\rho \left(\frac{\partial v^*}{\partial t^*} + u^* \frac{\partial v^*}{\partial x^*} - w_0^* \frac{\partial v^*}{\partial z^*} \right) = \mu \left(\frac{\partial^2 v^*}{\partial x^{*2}} + \frac{\partial^2 v^*}{\partial z^{*2}} \right) - \frac{\partial uv}{\partial x} - \frac{\delta \psi \mu_e^2 H_0^2 (v - mw)}{1 + m^2} \quad (18)$$

If electrical dissipation function and electromagnetic dissipation terms are neglected the energy equation becomes,

$$\frac{\partial T^*}{\partial t^*} + u^* \frac{\partial T^*}{\partial x^*} - w_0^* \frac{\partial T^*}{\partial z^*} = \frac{k}{\rho c_p} \left(\frac{\partial^2 T}{\partial x^{*2}} + \frac{\partial^2 T}{\partial z^{*2}} \right) + \phi + \frac{Q^+}{\rho c_p} \quad (19)$$

Finally the concentration equation is given by,

$$\frac{\partial C^*}{\partial t^*} + u^* \frac{\partial C^*}{\partial x^*} - w_0^* \frac{\partial C^*}{\partial z^*} = D \left(\frac{\partial^2 C^*}{\partial x^{*2}} + \frac{\partial^2 C^*}{\partial z^{*2}} \right) \quad (20)$$

Turbulent flow is defined as an eddying motion in which the various quantities show random variation with time and space coordinates, so that statistically distinct average values can be discerned (Hinze 1974, Reynolds 1976). The basic nature of turbulence can be described as a wide spectrum of various sized vortex elements which interact with each other in a highly random and unsteady fashion. That is

$$\rho = \bar{\rho} + \rho', \quad u_j = \bar{u}_j + u'_j, \quad p = \bar{p} + p'$$

Thus the continuity equation reduces to

$$\frac{\partial \bar{\rho}}{\partial t} + \frac{\partial}{\partial x_j} (\overline{\rho u_j}) + \frac{\partial}{\partial x_j} (\overline{\rho' u'_j}) = 0 \quad (21)$$

Averaging and adopting the Boussinesque approximation on the shear stress terms $\frac{\partial(\bar{u}^* \bar{v}^*)}{\partial x^*}$;

$$\frac{\partial(\bar{u}^* \bar{w}^*)}{\partial x^*}$$

$$\tau = -\rho \bar{v} \bar{w} = A \frac{\partial \bar{v}}{\partial z} \quad (24)$$

From experiment Prandtl deduced that;

$$\rho \bar{v} \bar{w} = -\rho l^2 \left(\frac{\partial \bar{v}}{\partial z} \right)^2 \quad (25)$$

Taking $l = kz$ where k is the Von Karman constant so we have;

$$\bar{u}^* \bar{v}^* = -k^2 x^2 \left(\frac{\partial \bar{v}^*}{\partial x^*} \right)^2 \quad (26)$$

$$\bar{u}^* \bar{w}^* = -k^2 x^2 \left(\frac{\partial \bar{w}^*}{\partial x^*} \right)^2 \quad (27)$$

Substituting in equations (17) and (18) we get

$$\frac{\partial \bar{u}^*}{\partial t^*} + \bar{u}^* \frac{\partial \bar{u}^*}{\partial x^*} - \bar{w}_0^* \frac{\partial \bar{u}^*}{\partial z^*} = \frac{\mu}{\rho} \left(\frac{\partial^2 \bar{u}^*}{\partial x^{*2}} + \frac{\partial^2 \bar{u}^*}{\partial z^{*2}} \right) + \beta(T^* - T_\infty^*)$$

$$+ \beta'(C^* - C_\infty^*) - \frac{\partial}{\partial x^*} \left[k^2 x^2 \left(\frac{\partial \bar{v}^*}{\partial x^*} \right)^2 \right] - \frac{\delta \psi \mu_e^2 H_0^2 (m v^* - w^*)}{\rho(1+m)^2} \quad (28)$$

$$\frac{\partial \bar{v}^*}{\partial t^*} + \bar{u}^* \frac{\partial \bar{v}^*}{\partial x^*} - \bar{w}_0^* \frac{\partial \bar{v}^*}{\partial z^*} = \frac{\mu}{\rho} \left(\frac{\partial^2 \bar{v}^*}{\partial x^{*2}} + \frac{\partial^2 \bar{v}^*}{\partial z^{*2}} \right)$$

$$- \frac{\partial}{\partial x^*} \left[k^2 x^2 \left(\frac{\partial \bar{w}^*}{\partial x^*} \right)^2 \right] - \frac{\delta \psi \mu_e^2 H_0^2 (v^* - m w^*)}{\rho(1+m)^2} \quad (29)$$

It is assumed that the induced magnetic field is negligible so that the fluid is permeated by a strong field $\vec{H} = (H_0 \sqrt{1-\psi^2}, 0, H_0 \psi)$ where $H_0 = |H|$ is the magnitude of the magnetic field and $\psi = \cos\theta$. This assumption hold for small magnetic Reynold's number. The equation of Electric charge $\nabla \cdot \mathbf{J} = 0$ gives $J_{z^*} = \text{constant}$; this constant is assumed to be zero, since $J_{z^*} = 0$ at the plate, which is electrically non-conducting. It implies that $J_{z^*} = 0$ everywhere in the flow.

Taking into consideration the Hall current (due to electrons), Ion-slip current (due to ions) and collisions between electrons and neutral particles, we obtain a modified Ohm's law of the form,

$$\mathbf{J} = \sigma [E + \mathbf{q} \times \mathbf{B}] - \frac{\omega_e \tau_e}{B_0} [\mathbf{J} \times \mathbf{B}] + \frac{\omega_e \tau_e \omega_i \tau_i}{B_0^2} (\mathbf{J} \times \mathbf{B}) \times \mathbf{B} \quad (30)$$

For short circuit problem the applied electric field $E = 0$.

Equation (30) becomes

$$\mathbf{J} = \sigma [\mathbf{q} \times \mathbf{B}] - \frac{\omega_e \tau_e}{B_0} [\mathbf{J} \times \mathbf{B}] + \frac{\omega_e \tau_e \omega_i \tau_i}{B_0^2} (\mathbf{J} \times \mathbf{B}) \times \mathbf{B} \quad (31)$$

Solving (31) for J_{x^*} and J_{y^*} yields,

$$J_{x^*} = \frac{\sigma \mu_e H_0 \psi [v^* (1 + m_* n_* \psi^2) + u^* m_* \psi]}{[1 + m_* n_* \psi^2]^2 + m_*^2 \psi^2} \quad (32)$$

$$J_{y^*} = \frac{\sigma \mu_e H_0 \psi [v^* m_* \psi - u^* (1 + m_* n_* \psi^2)]}{[1 + m_* n_* \psi^2]^2 + m_*^2 \psi^2} \quad (33)$$

Where $m_* = \omega_e \tau_e$ (Hall parameter) and $n_* = \omega_i \tau_i$ (Ion-slip parameter).

Substituting equation (32) and (33) in equation (28) and (29) from equations we obtain,

$$\rho \left(\frac{\partial u^*}{\partial t^*} + u^* \frac{\partial u^*}{\partial x^*} - w_0^* \frac{\partial u^*}{\partial z^*} \right) = \mu \left(\frac{\partial^2 u^*}{\partial x^{*2}} + \frac{\partial^2 u^*}{\partial z^{*2}} \right) + \beta \rho (T^* - T_\infty^*)$$

$$+ \beta' \rho (C^* - C_\infty^*) - \frac{\partial uv}{\partial x} + \frac{\sigma \mu_e^2 H_0^2 \psi^2 [v^* m_* \psi - u^* (1 + m_* n_* \psi^2)]}{[1 + m_* n_* \psi^2]^2 + m_*^2 \psi^2} \quad (34)$$

$$\rho \left(\frac{\partial v^*}{\partial t^*} + u^* \frac{\partial v^*}{\partial x^*} - w_0^* \frac{\partial v^*}{\partial z^*} \right) = \mu \left(\frac{\partial^2 v^*}{\partial x^{*2}} + \frac{\partial^2 v^*}{\partial z^{*2}} \right) - \frac{\partial uv}{\partial x}$$

$$- \frac{\sigma \mu_e^2 H_0^2 \psi^2 [v^* m_* \psi - u^* (1 + m_* n_* \psi^2)]}{[1 + m_* n_* \psi^2]^2 + m_*^2 \psi^2} \quad (35)$$

$$\frac{\partial T^*}{\partial t^*} + u^* \frac{\partial T^*}{\partial x^*} - w_0^* \frac{\partial T^*}{\partial z^*} = \frac{k}{\rho c_p} \left(\frac{\partial^2 T^*}{\partial x^{*2}} + \frac{\partial^2 T^*}{\partial z^{*2}} \right) + \frac{Q^*}{\rho c_p}$$

$$+ \frac{v}{\rho c_p} \left[\left(\frac{\partial u^*}{\partial x^*} \right)^2 + \left(\frac{\partial v^*}{\partial x^*} \right)^2 + \left(\frac{\partial u^*}{\partial z^*} \right)^2 + \left(\frac{\partial v^*}{\partial z^*} \right)^2 \right] \quad (36)$$

And

$$\frac{\partial C^*}{\partial t^*} + u^* \frac{\partial C^*}{\partial x^*} - w_0^* \frac{\partial C^*}{\partial z^*} = D \left(\frac{\partial^2 C^*}{\partial x^{*2}} + \frac{\partial^2 C^*}{\partial z^{*2}} \right) \quad (37)$$

IV. NON DIMENSIONALIZATION

The following non dimensional numbers are used in this paper;

A. Reynold's Number, Re

It is the ratio of inertia force to the viscous force acting on the fluid. If for any flow this number is less than one the inertia force is negligible and on the other hand if it is large, one can ignore viscous force and so the fluid can be taken as inviscid. It is given by

$$Re = \frac{\rho UL}{\mu} = \frac{UL}{\nu}$$

It plays a role in forced convection; its role is the same as that of Grashof number in natural/free convection.

Its critical value governs the transition from laminar to turbulent in forced convection.

B. PrandtlNumber, Pr

It is the ratio of viscous force to thermal force acting on the fluid. It relates the velocity field with temperature field, and is the ratio of the transport properties ν and α , which govern the transport of momentum and energy respectively. It plays a role in heat transfer.

The Prandtl number is large when thermal conductivity is less than one and viscosity is large, and is small when viscosity is less than one and thermal conductivity is large.

$$Pr = \frac{\nu}{\alpha} ; \quad \alpha = \frac{k}{\rho c}$$

ν – momentum (kinematic diffusivity)

α – thermal diffusivity

Or $Pr = \frac{\mu c_p}{k}$

C. GrashofNumber, Gr

This is another non-dimensional number, which usually occurs in natural convection problems. It is due to density differences resulting from concentration difference and not temperature differences and defined as the ratio of buoyancy forces to viscous forces acting on the fluid. Its critical value governs the transition from laminar to turbulent flow in natural/free convection.

The larger it is the stronger is the convective current.

$$Gr = \frac{\nu g \beta (T_w^* - T_\infty^*)}{U^3}$$

D. Eckert Number, Ec

This is the ratio of the kinetic energy to thermal energy.

$$Ec = \frac{U^2}{c_p (T_w^* - T_\infty^*)}$$

E. Hartmann Number, M

It is the ratio of magnetic force to the viscous force,

$$M^2 = \frac{\sigma \mu_e^2 H_0^2 \nu}{U \rho}$$

F. Schmidt Number, Sc

This provides a measure of the relative effectiveness of momentum and mass transport by diffusion in the velocity field and concentration boundary layers respectively.

It relates the velocity field with the concentration field, and is the ratio of the transport properties ν and D , which govern the transport of momentum and mass respectively.

Plays a role in mass transfer; its role in mass transfer is the same as that of Prandtl number in heat transfer.

$$Sc = \frac{\nu}{D}$$

ν – momentum (kinematic) diffusivity

D – mass diffusivity

G. NusseltNumber, Nu

This parameter is equal to the dimensionless temperature gradient at the surface. It provides a measure of the convection heat transfer occurring at the surface.

$$Nu = \frac{\delta \theta}{\delta x} \Big|_{x=0}$$

H. Sherwood Number, Sh

Is the dimensionless concentration gradient at the surface. It provides a measure of the convection mass transfer occurring at the surface.

$$Sh = \frac{\delta C}{\delta x} \Big|_{x=0}$$

In this study, all the variables with the superscript (*) star will represent dimensional variables and non-dimensionalization is based on the following sets of scaling variables.

On introducing the dimensionless quantities

$$t = \frac{t^* U^2}{\nu}, \quad x = \frac{x^* U}{\nu}, \quad z = \frac{z^* U}{\nu}, \quad u = \frac{u^*}{U}, \quad v = \frac{v^*}{U}, \quad w_0 = \frac{w_0^*}{U},$$

$$\tau = \frac{\tau^*}{\rho U}, \quad \theta = \frac{T^* - T_\infty^*}{T_w^* - T_\infty^*}, \quad C = \frac{C^* - C_\infty^*}{C_w^* - C_\infty^*}, \quad Sc = \frac{D}{\nu}, \quad \delta = \frac{Q\nu}{kU^2},$$

$$Gr = \frac{\nu g \beta (T_w^* - T_\infty^*)}{U^3}, \quad Gc = \frac{\nu g \beta' (C_w^* - C_\infty^*)}{U^3} \tag{38}$$

Equations (34) to (37) becomes,

$$\frac{\partial u}{\partial t} + u \frac{\partial u}{\partial x} - w_0 \frac{\partial u}{\partial z} = \left(\frac{\partial^2 u}{\partial x^2} + \frac{\partial^2 u}{\partial z^2} \right) + Gr\theta + GcC$$

$$- \left[2k^2 x \left(\frac{\partial v}{\partial x} \right)^2 + 2k^2 x^2 \left(\frac{\partial^2 v}{\partial x^2} \right) \left(\frac{\partial v}{\partial x} \right) \right] + \frac{M^2 \psi^2 [v m_* \psi - u(1 + m_* n_* \psi^2)]}{[1 + m_* n_* \psi^2]^2 + m_*^2 \psi^2} \tag{39}$$

$$\frac{\partial v}{\partial t} + u \frac{\partial v}{\partial x} - w_0 \frac{\partial v}{\partial z} = \left(\frac{\partial^2 v}{\partial x^2} + \frac{\partial^2 v}{\partial z^2} \right) - \left[2k^2 x \left(\frac{\partial v}{\partial x} \right)^2 + 2k^2 x^2 \left(\frac{\partial^2 v}{\partial x^2} \right) \left(\frac{\partial v}{\partial x} \right) \right]$$

$$- \frac{M^2 \psi^2 [u m_* \psi + v(1 + m_* n_* \psi^2)]}{[1 + m_* n_* \psi^2]^2 + m_*^2 \psi^2} \tag{40}$$

$$\frac{\partial \theta}{\partial t} + u \frac{\partial \theta}{\partial x} - w_0 \frac{\partial \theta}{\partial z} = \frac{1}{Pr} \left[\frac{\partial^2 \theta}{\partial x^2} + \frac{\partial^2 \theta}{\partial z^2} \right] - \frac{\sigma}{Pr} \theta + Ec \left[\left(\frac{\partial u}{\partial x} \right)^2 + \left(\frac{\partial v}{\partial x} \right)^2 + \left(\frac{\partial u}{\partial z} \right)^2 + \left(\frac{\partial v}{\partial z} \right)^2 \right] \tag{41}$$

and

$$\frac{\partial C}{\partial t} + u \frac{\partial C}{\partial x} - w_0 \frac{\partial C}{\partial z} = \frac{1}{Sc} \left(\frac{\partial^2 C}{\partial x^2} + \frac{\partial^2 C}{\partial z^2} \right)$$

Initial and boundary conditions in non-dimensional form are,
For

$$\left. \begin{aligned} t > 0, u(\infty, x, t) = 0, v(\infty, x, t) = 0 \\ \theta(\infty, x, t) = 0, C(\infty, x, t) = 0 \end{aligned} \right\} \quad (43)$$

For

$$\left. \begin{aligned} t \leq 0, u(z, x, 0) = 0, v(z, x, 0) = 0 \\ \theta(z, x, 0) = 0, C(z, x, 0) = 0 \end{aligned} \right\}$$

V. METHOD OF SOLUTION

Equations (39) to (42) are highly non-linear and therefore exact solutions are not possible, in order to solve these equations a fast and stable method for the solution of finite difference approximation has been developed together with the initial and boundary condition (43) to (45). The profiles given by $u_{(k,i)}^{n+1}$, $v_{(k,i)}^{n+1}$, $\theta_{(k,i)}^{n+1}$ and $C_{(k,i)}^{n+1}$ are computed by the following algorithms,

$$u_{(k,i)}^{n+1} = \Delta t \left\{ \begin{aligned} & -u_{(k,i)}^n \left[\frac{u_{(k,i+1)}^n - u_{(k,i-1)}^n}{2\Delta x} \right] + w_0 \left[\frac{u_{(k+1,i)}^n - u_{(k-1,i)}^n}{2\Delta z} \right] + \frac{u_{(k+1,i)}^n - 2u_{(k,i)}^n + u_{(k-1,i)}^n}{(\Delta z)^2} \\ & + \frac{u_{(k,i+1)}^n - 2u_{(k,i)}^n + u_{(k,i-1)}^n}{(\Delta x)^2} + Gr\theta_{(k,i)}^n + GcC_{(k,i)}^n - 2k^2 i \Delta x \left(\frac{u_{(k,i+1)}^n - 2u_{(k,i)}^n + u_{(k,i-1)}^n}{2\Delta x} \right)^2 \\ & - 2k^2 (i\Delta x)^2 \left(\frac{u_{(k,i+1)}^n - 2u_{(k,i)}^n + u_{(k,i-1)}^n}{(\Delta x)^2} \right)^2 \left(\frac{u_{(k,i+1)}^n - u_{(k,i)}^n}{2\Delta x} \right) \\ & - \frac{M^2 \psi^2 [v_{(k,i)}^n m_* \psi - u_{(k,i)}^n (1 + m_* n_* \psi^2)]}{[1 + m_* n_* \psi^2]^2 + m_*^2 \psi^2} \end{aligned} \right\} + u_{(k,i)}^n \quad (46)$$

$$v_{(k,i)}^{n+1} = \Delta t \left\{ \begin{aligned} & -v_{(k,i)}^n \left[\frac{v_{(k,i+1)}^n - v_{(k,i-1)}^n}{2\Delta x} \right] + w_0 \left[\frac{v_{(k+1,i)}^n - v_{(k-1,i)}^n}{2\Delta z} \right] + \frac{v_{(k+1,i)}^n - 2v_{(k,i)}^n + v_{(k-1,i)}^n}{(\Delta z)^2} \\ & + \frac{v_{(k,i+1)}^n - 2v_{(k,i)}^n + v_{(k,i-1)}^n}{(\Delta x)^2} - 2k^2 i \Delta x \left(\frac{v_{(k,i+1)}^n - 2v_{(k,i)}^n + v_{(k,i-1)}^n}{2\Delta x} \right)^2 \\ & - 2k^2 (i\Delta x)^2 \left(\frac{v_{(k,i+1)}^n - 2v_{(k,i)}^n + v_{(k,i-1)}^n}{(\Delta x)^2} \right)^2 \left(\frac{v_{(k,i+1)}^n - v_{(k,i)}^n}{2\Delta x} \right) \\ & - \frac{M^2 \psi^2 [u_{(k,i)}^n m_* \psi + v_{(k,i)}^n (1 + m_* n_* \psi^2)]}{[1 + m_* n_* \psi^2]^2 + m_*^2 \psi^2} \end{aligned} \right\} + v_{(k,i)}^n \quad (47)$$

$$\begin{aligned} & \frac{\theta_{(k,i)}^{n+1} - \theta_{(k,i)}^n}{\Delta t} + u_{(k,i)}^n \left[\frac{\theta_{(k,i+1)}^n - \theta_{(k,i-1)}^n}{2\Delta x} \right] - w_0 \frac{\theta_{(k+1,i)}^n - \theta_{(k-1,i)}^n}{2\Delta z} = \frac{1}{Pr} \left[\frac{\theta_{(k,i+1)}^n - 2\theta_{(k,i)}^n + \theta_{(k,i-1)}^n}{(\Delta x)^2} \right] \\ & + \frac{1}{Pr} \left[\frac{\theta_{(k+1,i)}^n - 2\theta_{(k,i)}^n + \theta_{(k-1,i)}^n}{(\Delta z)^2} \right] - \frac{\sigma}{Pr} \theta_{(k,i)}^n + Ec \left[\begin{aligned} & \left(\frac{u_{(k,i+1)}^n - u_{(k,i-1)}^n}{2\Delta x} \right)^2 + \left(\frac{v_{(k,i+1)}^n - v_{(k,i-1)}^n}{2\Delta x} \right)^2 \\ & + \left(\frac{u_{(k+1,i)}^n - u_{(k-1,i)}^n}{2\Delta z} \right)^2 + \left(\frac{v_{(k+1,i)}^n - v_{(k-1,i)}^n}{2\Delta z} \right)^2 \end{aligned} \right] + \theta_{(k,i)}^n \quad (48)
 \end{aligned}$$

$$\theta_{(k,i)}^{n+1} = \Delta t \left\{ -u_{(k,i)}^n \left[\frac{\theta_{(k,i+1)}^n - \theta_{(k,i-1)}^n}{2\Delta x} \right] + w_0 \left[\frac{\theta_{(k+1,i)}^n - \theta_{(k-1,i)}^n}{2\Delta z} \right] + \frac{1}{Pr} \frac{\theta_{(k+1,i)}^n - 2\theta_{(k,i)}^n + \theta_{(k-1,i)}^n}{(\Delta z)^2} \right. \\ \left. + \frac{1}{Pr} \frac{\theta_{(k,i+1)}^n - 2\theta_{(k,i)}^n + \theta_{(k,i-1)}^n}{(\Delta x)^2} - \frac{\sigma}{Pr} \theta_{(k,i)}^n + Ec \left[\left(\frac{u_{(k,i+1)}^n - u_{(k,i-1)}^n}{2\Delta x} \right)^2 + \left(\frac{v_{(k,i+1)}^n - v_{(k,i-1)}^n}{2\Delta x} \right)^2 \right] \right\} + \theta_{(k,i)}^n \\ \left[+ \left(\frac{u_{(k+1,i)}^n - u_{(k-1,i)}^n}{2\Delta z} \right)^2 + \left(\frac{v_{(k+1,i)}^n - v_{(k-1,i)}^n}{2\Delta z} \right)^2 \right]$$

And

(49)

$$C_{(k,i)}^{n+1} = \Delta t \left\{ -u_{(k,i)}^n \left[\frac{C_{(k,i+1)}^n - C_{(k,i-1)}^n}{2\Delta x} \right] + w_0 \left[\frac{C_{(k+1,i)}^n - C_{(k-1,i)}^n}{2\Delta z} \right] + \frac{1}{Sc} \left[\left(\frac{C_{(k,i+1)}^n - 2C_{(k,i)}^n + C_{(k,i-1)}^n}{2\Delta x} \right) + \left(\frac{C_{(k+1,i)}^n - 2C_{(k,i)}^n + C_{(k-1,i)}^n}{2\Delta z} \right)^2 \right] \right\} + C_{(k,i)}^n$$

A. Calculation Of Rates Of Heat Transfer, Mass Transfer And Skin Friction

1. The skin friction is calculated from velocity profiles using the equations

$$\left\{ \tau_x = -\frac{\partial u}{\partial z} \Big|_{z=0} \quad \text{and} \quad \tau_y = -\frac{\partial v}{\partial z} \Big|_{z=0} \quad \text{where} \quad \tau = \frac{\tau^*}{\rho\mu^2} \right\} \quad (51)$$

2. Rate of mass transfer is calculated from the concentration profile using the equation,

$$Sh = -\frac{\partial C}{\partial z} \Big|_{z=0} \quad (52)$$

The above are calculated by numerical differentiation using Newton's interpolation formula over the first five points,

$$\tau_x = \frac{5}{6} [25u(0, i) - 48u(1, i) + 36u(2, i) - 16u(3, i) + 3u(4, i)] \quad (53)$$

$$\tau_y = \frac{5}{6} [25v(0, i) - 48v(1, i) + 36v(2, i) - 16v(3, i) + 3v(4, i)] \quad (54)$$

$$Sh = \frac{5}{6} [25C(0, i) - 48C(1, i) + 36C(2, i) - 16C(3, i) + 3C(4, i)] \quad (55)$$

The rate of heat transfer is calculated from temperature profiles in terms of the Nusselt number which is given by,

$$Nu = -\frac{1}{\theta_{(0,0)}^{n+1}} \frac{\partial \theta}{\partial z} \Big|_{z=0}$$

But $\frac{\partial \theta}{\partial z} = -1$ which implies that

$$Nu = \frac{1}{\theta_{(0,0)}^{n+1}} \quad (56)$$

VI. DISCUSSION OF RESULTS

A program was written and run for various values of velocities, temperatures and concentration for the finite differences equations (34) to (37) using different values of the parameters $Sc, m, n, \sigma, wo, t, Gc, Ec$ and ψ . The velocities are classified as primary velocities (u) and secondary velocities (v) along the x and y axes respectively.

The concentration, velocity and temperature profiles are presented graphically in figures. Grashof number $Gr > 0, (+0.4)$ corresponding to cooling of the plate by free convection currents and Grashof number $Gr < 0, (-0.4)$ corresponds to heating of the plate by free convection currents. The magnetic parameter $M^2 = 5.0$ signifies a strong magnetic field and Prandtl number $Pr = 0.71$ corresponds to air.

Figures and tables for $Pr = 0.71, M^2 = 5.0, Gr = +0.4$

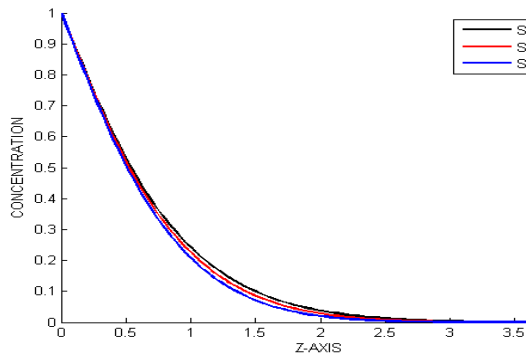


Figure 6.3a: Variation of concentration with Schmidt number Sc , with ion-slip

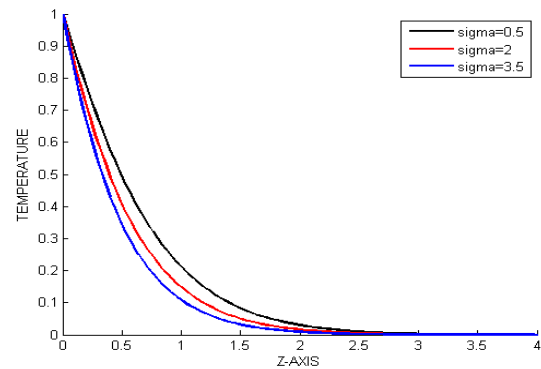


Figure 6.4a: Variation of Temperature with heat source parameter σ , with ion-slip

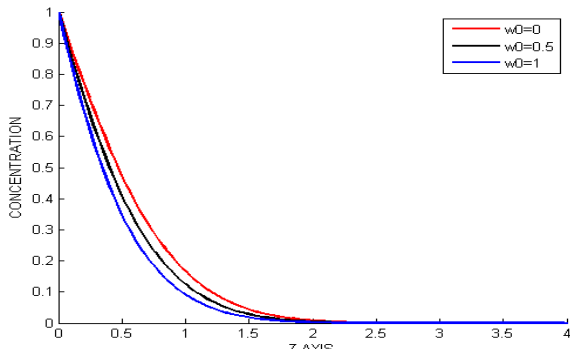


Figure 6.3b: Variation of concentration with Suction velocity w_0 , with ion-slip

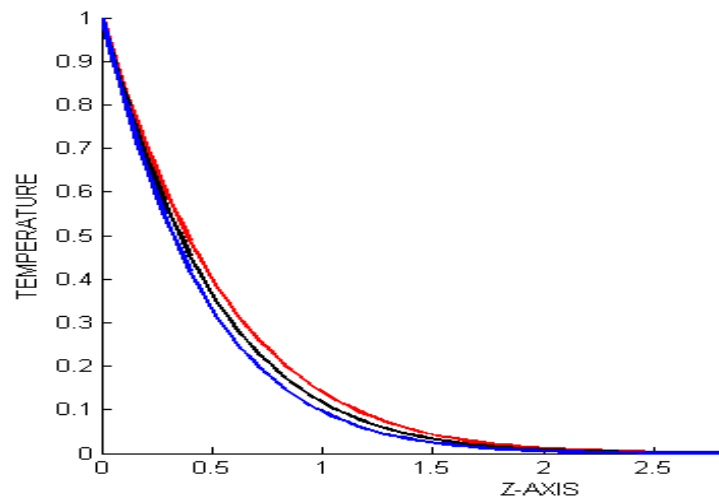


Figure 6.4b: Variation of Temperature with suction velocity w_0 , with ion-slip

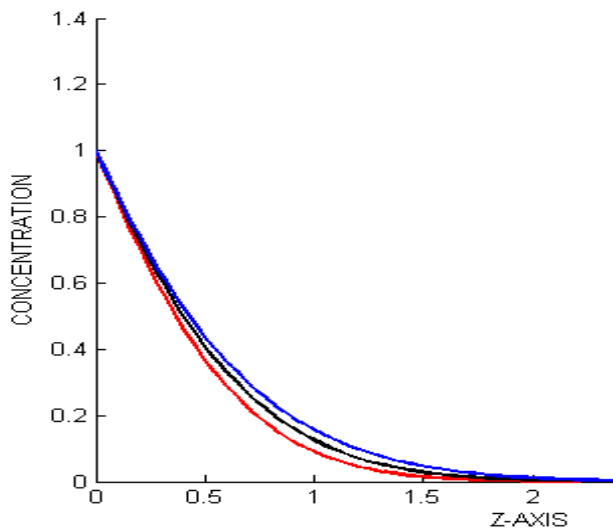


Figure 6.3c: Variation of concentration with time t , with ion-slip

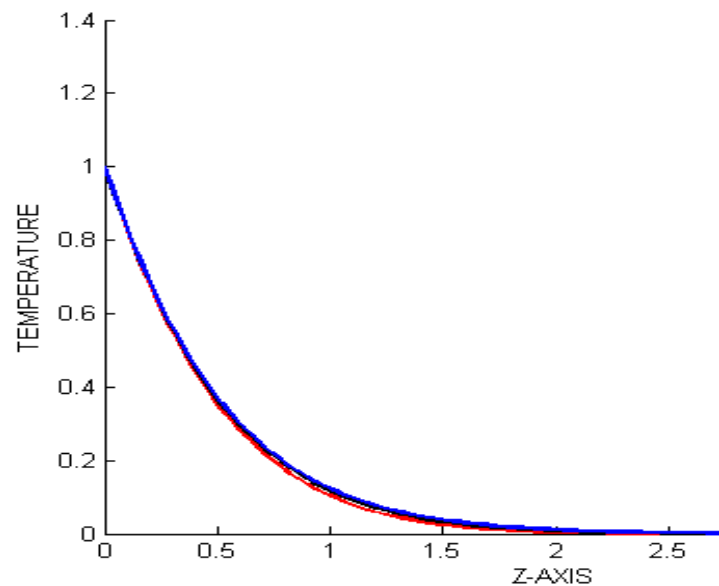


Figure 6.4c: Variation of Temperature with time t , with ion-slip

From figure 6.3a - 6.3c; $Gr > 0, (+0.4)$, with ion-slip (n); we note that;

- i.) An increase in mass diffusion parameter Sc causes a decrease in the concentration profiles (figure 6.3a)
- ii.) Removal of suction velocity w_0 leads to an increase in the concentration profiles. This is due to the fact that this increases the growth of the boundary layers and hence the increase in the concentration profiles (figure 6.3b)
- iii.) Increase in time increases the concentration profiles. With time the flow gets to the free stream and therefore its concentration increases (figure 6.3c)

From figure 6.4a-6.4c; $Gr > 0, (+0.4)$, with ion-slip (n); we note that;

- i.) An increase in time t or a decrease in heat source parameter σ leads to an increase in

temperature profiles

- ii.) Removal of suction velocity w_0 causes increase in temperature profiles.
- ii.) Angle of inclination ψ causes no effect in temperature profiles
- iii.) An increase in ion-slip parameter n causes no effect in temperature profiles
- iv.) An increase in Hall parameter m leads to no effect in temperature profiles
- v.) An increase in mass diffusion parameter Sc causes no effect in temperature profiles.

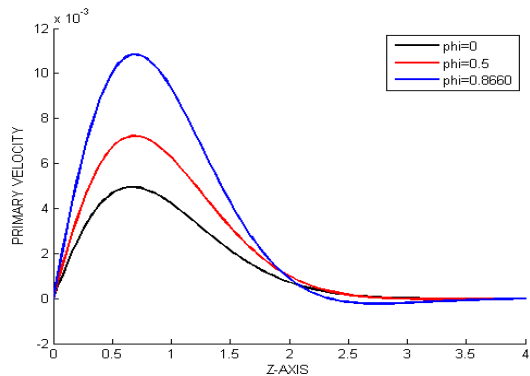


Figure 6.5 a: Variation of Primary velocity with angle of inclination ψ , with ion-slip

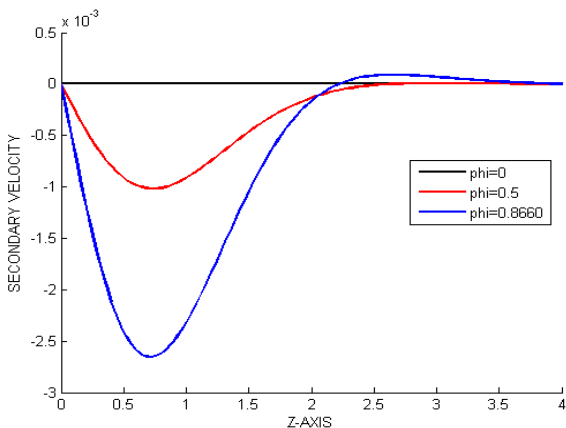


Figure 6.5 b: Variation of Secondary velocity with angle of inclination ψ , with ion-slip

From figure 6.5 a and 6.5 b; $Gr > 0, (+0.4)$ with ion-slip (n); we note that;

An increase in the angle of inclination ψ causes an increase in primary velocity profiles and a decrease in secondary profiles near the plate but away from the plate it decreases primary velocity but increase in secondary velocity to a point where both remain uniformly distributed.

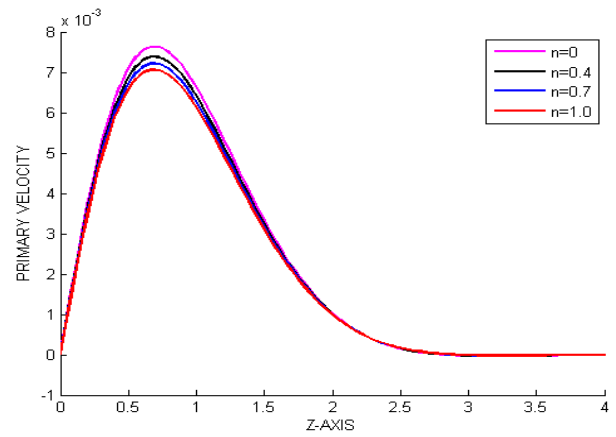


Figure 6.6 a: Variation of Primary velocity with ion-slip n

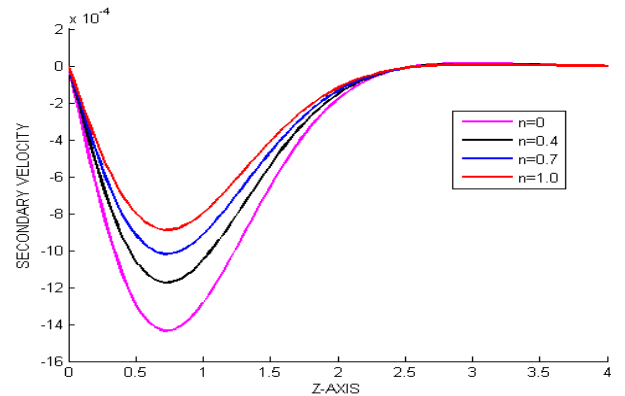


Figure 6.6 b: Variation of Secondary velocity with ion-slip n

From figure 6.6 a and 6.6 b; $Gr > 0, (+0.4)$ with ion-slip (n); we note that;

An increase in ion-slip parameter n leads to a negligible increase in primary velocity profiles but a decrease in secondary velocity profiles near the plate and remain constantly distributed away from the plate, this is because increase in ion-slip currents cause the force in the direction of the fluid flow to decrease leading to a decrease in the secondary velocity of the fluid. Since the magnitude of secondary velocity profile is very small, there is a very small increase in primary velocity profile with the change in the ion-slip currents.

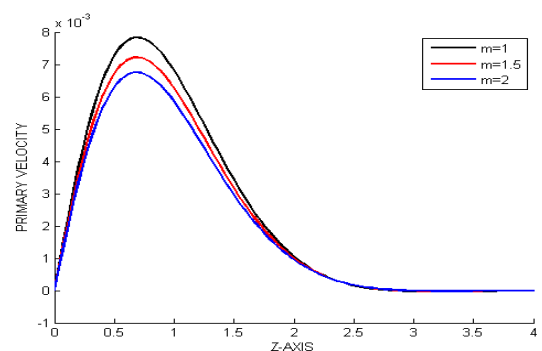


Figure 6.7 a: Variation of Primary velocity with Hall parameter m , with ion-slip:

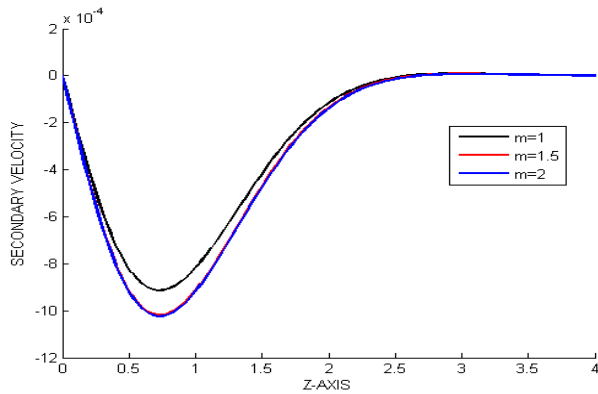


Figure 6.7 b: Variation of Secondary velocity with Hall parameter m , with ion-slip:

From figure 6.7 a and 6.7 b; $Gr > 0, (+0.4)$ with ion-slip (n); we note that; An increase in Hall current parameter m causes a decrease in both primary and secondary velocity profiles.

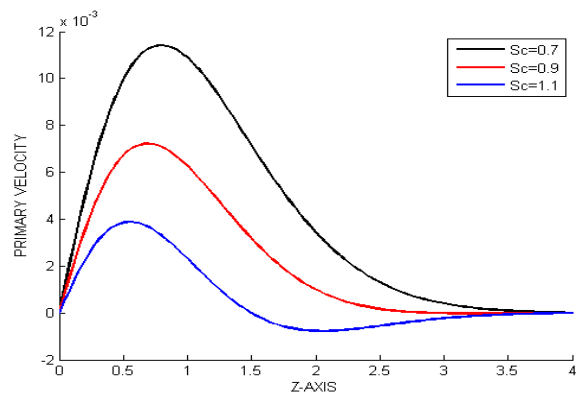


Figure 6.8 a: Variation of Primary velocity with Schmidt number Sc , with ion-slip

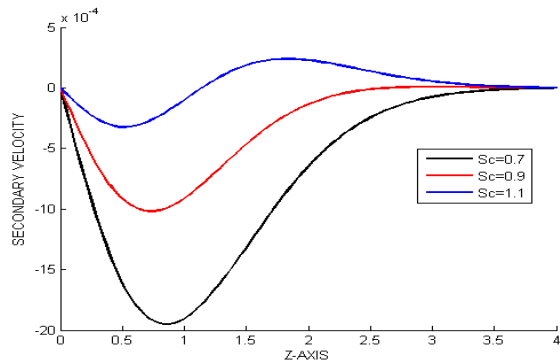


Figure 6.8 b: Variation of Secondary velocity with Schmidt number Sc , with ion-slip

From figure 6.8 a and 6.8 b; $Gr > 0, (+0.4)$ with ion-slip (n); we note that; An increase in mass diffusion parameter Sc leads to a decrease in primary velocity profiles but an increase in secondary velocity profiles near the plate and the velocity profiles remain constantly distributed far away from the plate.

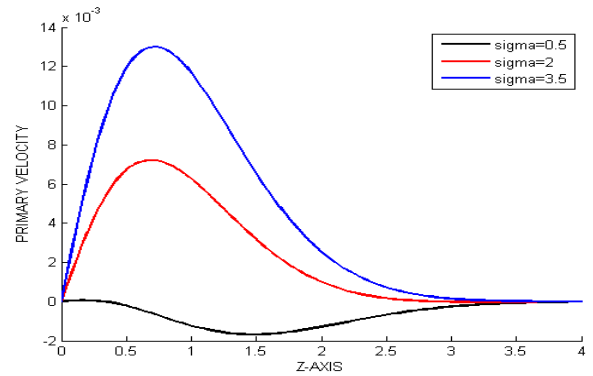


Figure 6.9 a: Variation of Primary velocity with heat source parameter σ , with ion-slip

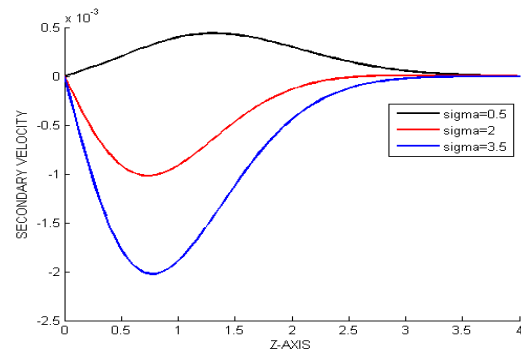


Figure 6.9 b: Variation of Secondary velocity with heat source parameter σ , with ion-slip

From figure 6.5 a and 6.5 b; $Gr > 0, (+0.4)$ with ion-slip (n); we note that;

An increase in heat source parameter σ leads to a decrease in primary velocity profiles but an increase in secondary velocity profiles near the plate and thereafter remain constantly distributed far away from the plate .

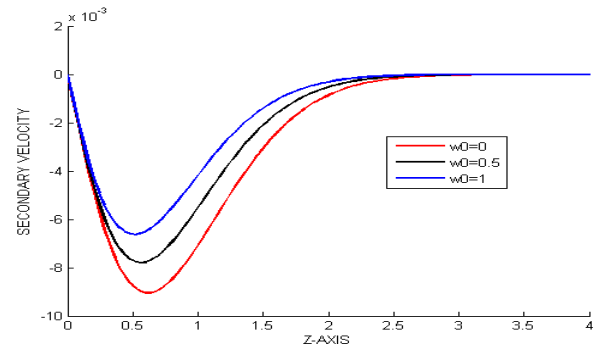


Figure 7.0a: Variation of Secondary velocity with suction velocity w_0 , with ion-slip

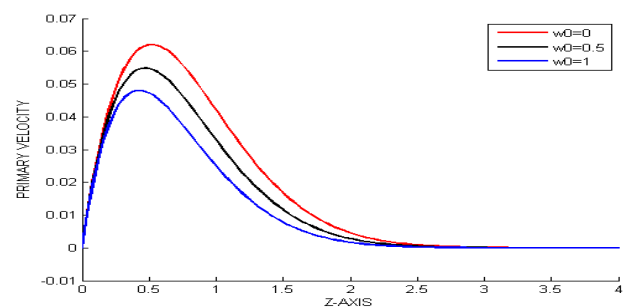


Figure 7.0b: Variation of Primary velocity with suction velocity w_0 , with ion-slip

From the figures 7.0a and 7.0b, we observe that; i.) Removal of suction velocity w_0 leads to a gradual

increase in primary velocity profiles near the plate to a maximum point after which the primary velocity profiles begin decrease uniformly then remain constantly distributed far away from the plate in the free stream (figure 7.0b)

ii.) Removal of suction velocity w_0 leads to a gradual decrease in secondary velocity profiles near the plate to a maximum after which the secondary profiles velocity profiles begin to increase gradually then remain constantly distributed far away from the plate in the free streams

(Figure 7.0a)

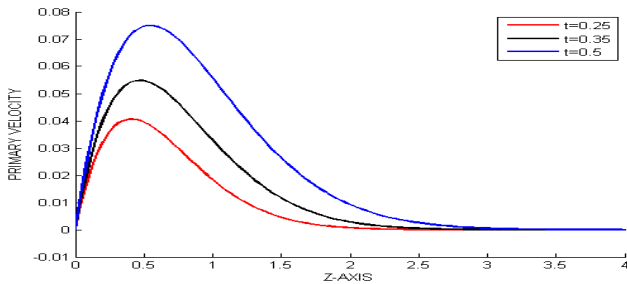


Figure 7.1a: Variation of Primary velocity with time t , with ion-slip

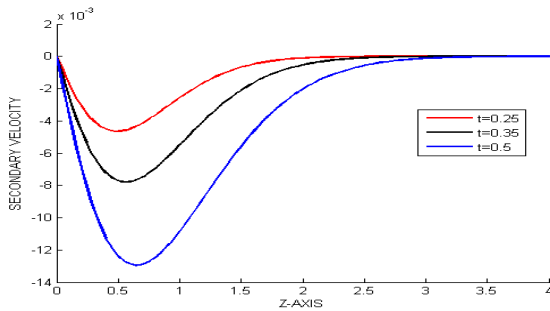


Figure 7.1b: Variation of Secondary velocity with time t , with ion-slip

From the figures 7.1a and 7.1b,we observe that;

i.) An increase in time t increases the primary velocity profiles. With time the flow gets to the free stream and therefore its velocity increases (figure 7.1a)

ii.) An increase in time t decreases the secondary velocity profiles. With time the flow gets to the free stream where the secondary velocity diminishes and therefore decrease in velocity profiles (figure 7.1b)

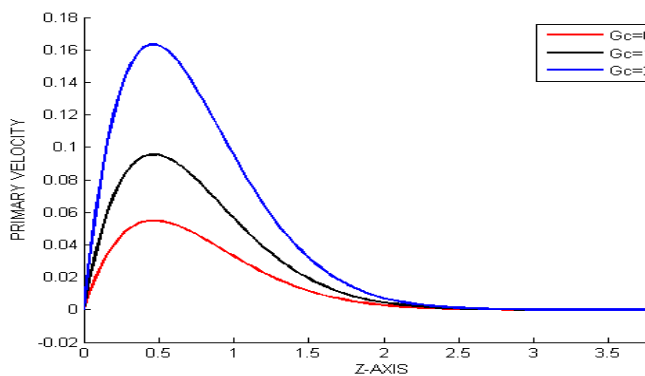


Figure 7.2a: Variation of Primary velocity with Modified Grashof G_c , with ion-slip

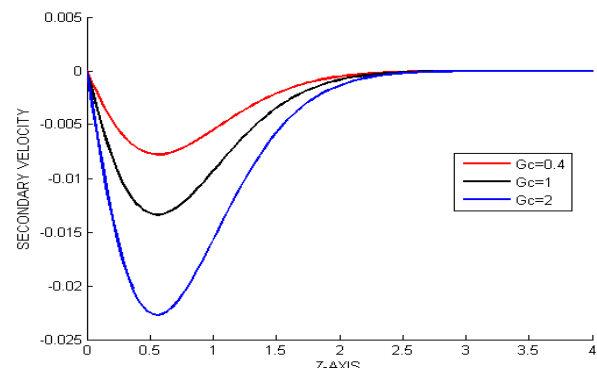
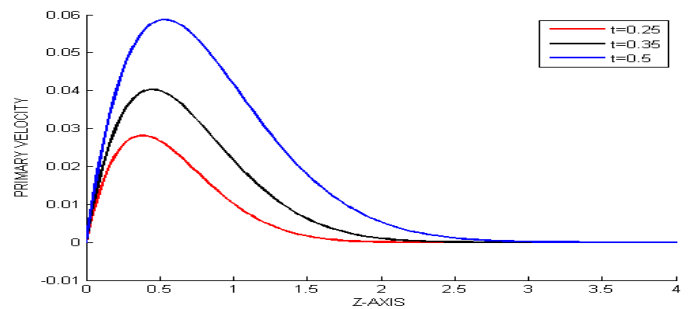


Figure 7.2b: Variation of Secondary velocity with Modified Grashof G_c , with ion-slip

From the figures 7.1a and 7.1b,we observe that;

i.) An increase in the Modified Grashof parameter G_c leads to a gradual increase in primary velocity profiles near the plate to a maximum after which the profiles begin to decrease gradually to a point in the free stream where the distribution remain constant and parallel to the z axis.

ii.) An increase in the Modified Grashof parameter G_c leads to a gradual decrease in secondary velocity profiles near the plate to a minimum after which the profiles begin to



increase gradually to a point in the free stream where the distribution remain constant and parallel to the z axis.

Figure 7.3a: Variation of Primary velocity with time t , $Gr = -0.4$, with ion-slip

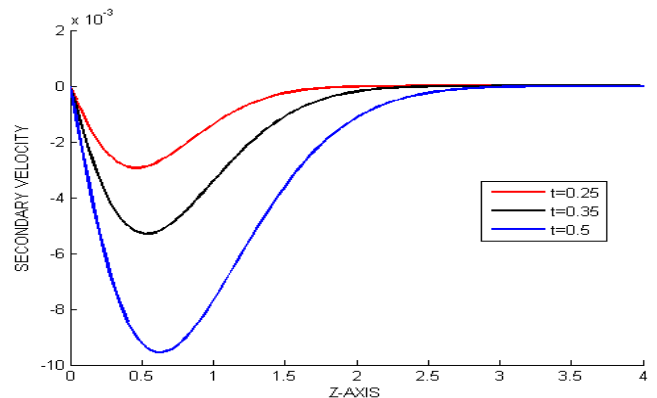


Figure 7.3b: Variation of Secondary velocity with time t , $Gr = -0.4$, with ion-slip

From figures 7.3a to 7.3b,we observe that;

An increase in time t leads to an increase in primary velocity profiles but a decrease in secondary velocity profiles from the curves $t = 0.25$ to $t = 0.5$ and $t = 0.5$ to 0.25 respectively near the plate and the velocity remain constantly distributed far away from the plate.

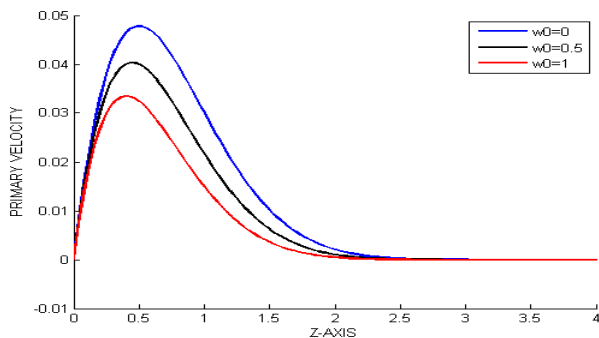


Figure 7.4a: Variation of Primary velocity with Suction velocity w_0 , $Gr = -0.4$, with ion-slip

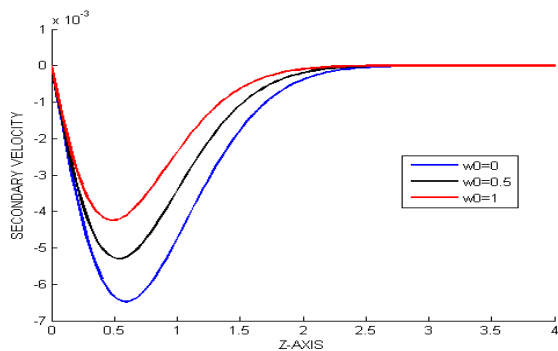


Figure 7.4b: Variation of Secondary velocity with Suction velocity w_0 , $Gr = -0.4$, with ion-slip

From figures 7.4a and 7.4b, we observe that;

- i.) An increase in Hall parameter or removal of suction velocity w_0 causes an increase in primary velocity profiles, this due to the fact that the effective conductivity decreases with the increase in Hall current parameter or removal of suction velocity which reduces the magnetic damping force hence the increase in primary velocity profiles.
- ii.) An increase in Hall current parameter or removal of suction velocity profile causes a decrease in secondary velocity profiles, this is due to increase in the effective

conductivity which increases the magnetic damping force hence the decrease in secondary velocity profiles.

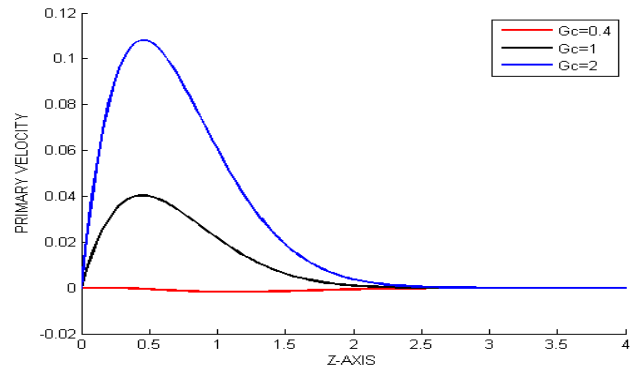


Figure 7.5a: Variation of Primary velocity with Modified Grashof G_c , $Gr = -0.4$, with ion-slip

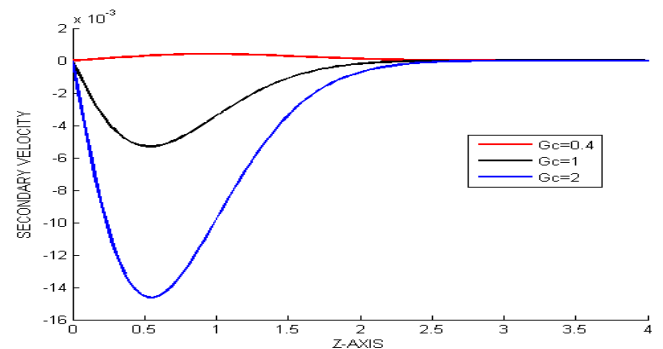


Figure 7.5 b: Variation of Secondary velocity with Modified Grashof G_c , $Gr = -0.4$, with ion-slip

From figures 7.5a and 7.5b, we observe that;

- i.) An increase in modified Grashof number G_c causes an increase in primary velocity profiles but as the distance from the plate increases primary velocity profiles exhibit a decrease and remain parallel to the z -axis far away from the plate.
- ii.) An increase in modified Grashof number G_c causes a decrease in secondary velocity profiles but as the distance from the plate increase secondary velocity profiles exhibit an increase gradually and remain parallel to the z -axis far away from the plate.

Table 5.1 Rate of mass transfer, $Pr = 0.71$, $M^2 = 5.0$, $Gr = +0.4$

w_0	Sc	Time	Sh
0	1.1	0.25	2.1109
0.5	1.1	0.25	2.3356
1	1.1	0.25	2.5862
0.5	0.7	0.25	2.202
0.5	0.9	0.25	2.2672
0.5	1.1	0.25	2.3356
0.5	1.1	0.25	2.3958
0.5	1.1	0.35	2.3356
0.5	1.1	0.5	2.295

From Table 5.1, we observe that;

- i.) Removal of suction velocity w_0 causes a decrease in rate of mass transfer Sh
- ii.) Increase in the mass diffusion parameter Sc , leads to an increase in rate of mass transfer Sh
- iii.) Increase in time t leads to a decrease in rate of mass transfer Sh

Table 5.2 : Values of skin friction, τ_x and τ_y for

$Pr = 0.71, M^2 = 5.0, Gr = 0.4$

n	w_0	m	Gc	Sc	Sigma a	Phi	Time	τ_x	τ_y
0	0.5	1.5	0.4	1.1	2	0.5	0.35	-0.1732	0.02
0.5	0.5	1.5	0.4	1.1	2	0.5	0.35	-0.1689	0.0155
1	0.5	1.5	0.4	1.1	2	0.5	0.35	-0.1652	0.0123
0.7	0	1.5	0.4	1.1	2	0.5	0.35	-0.1674	0.0141
0.7	0.5	1.5	0.4	1.1	2	0.5	0.35	-0.1673	0.0141
0.7	1	1.5	0.4	1.1	2	0.5	0.35	-0.1653	0.0138
0.7	0.5	1	0.4	1.1	2	0.5	0.35	-0.176	0.0127
0.7	0.5	1.5	0.4	1.1	2	0.5	0.35	-0.1676	0.0141
0.7	0.5	2	0.4	1.1	2	0.5	0.35	-0.1609	0.0141
0.7	0.5	1.5	0.4	1.1	2	0.5	0.35	-0.1673	0.0141
0.7	0.5	1.5	1	1.1	2	0.5	0.35	-0.2932	0.0244
0.7	0.5	1.5	2	1.1	2	0.5	0.35	-0.503	0.0417
0.7	0.5	1.5	0.4	0.7	2	0.5	0.35	-0.1763	0.0155
0.7	0.5	1.5	0.4	0.9	2	0.5	0.35	-0.1715	0.0147
0.7	0.5	1.5	0.4	1.1	2	0.5	0.35	-0.1673	0.0141
0.7	0.5	1.5	0.4	1.1	0.5	0.5	0.35	-0.174	0.0749
0.7	0.5	1.5	0.4	1.1	2	0.5	0.35	-0.1673	0.0141
0.7	0.5	1.5	0.4	1.1	3.5	0.5	0.35	-0.1619	0.0135
0.7	0.5	1.5	0.4	1.1	2	0	0.35	-0.1363	0
0.7	0.5	1.5	0.4	1.1	2	0.5	0.35	-0.1673	0.0141
0.7	0.5	1.5	0.4	1.1	2	0.87	0.35	-0.2258	0.04
0.7	0.5	1.5	0.4	1.1	2	0.5	0.25	-0.1457	0.0097
0.7	0.5	1.5	0.4	1.1	2	0.5	0.35	-0.1673	0.0141
0.7	0.5	1.5	0.4	1.1	2	0.5	0.5	-0.1942	0.0204

From table 5.2, we observe that;

- i.) An increase in modified Grashof number Gc or an increase in Hall parameter m leads to a decrease in skin friction τ_x and an increase in skin friction τ_y .
- ii.) An increase in the mass diffusion parameter Sc leads to an increase in skin friction τ_x but a decrease in skin friction τ_y .
- iii.) A decrease in heat source parameter σ or an increase in time t causes a decrease in skin friction

τ_x and an increase in skin friction τ_y . The removal of suction velocity w_0 causes a decrease in skin friction τ_x and an increase in skin friction τ_y .

iv.) An increase in the angle of inclination ψ and ion-slip parameter n leads to a decrease in both skin frictions τ_x and τ_y .

Table 5.3 Rate of Convection heat transfer Nu , $Pr = 0.71, M^2 = 5.0, Gr = + 0.4$

n	w_0	m	Gc	Sc	Sigma	Phi	Time	Nu
0	0.5	1.5	0.4	1.1	2	0.5	0.35	2.5488
0.5	0.5	1.5	0.4	1.1	2	0.5	0.35	2.5488
1	0.5	1.5	0.4	1.1	2	0.5	0.35	2.5488
0.7	0	1.5	0.4	1.1	2	0.5	0.35	2.4073
0.7	0.5	1.5	0.4	1.1	2	0.5	0.35	2.5488
0.7	1	1.5	0.4	1.1	2	0.5	0.35	2.7002
0.7	0.5	1	0.4	1.1	2	0.5	0.35	2.5488
0.7	0.5	1.5	0.4	1.1	2	0.5	0.35	2.5488
0.7	0.5	2	0.4	1.1	2	0.5	0.35	2.5488
0.7	0.5	1.5	0.4	1.1	2	0.5	0.35	2.5488
0.7	0.5	1.5	1	1.1	2	0.5	0.35	2.5488
0.7	0.5	1.5	2	1.1	2	0.5	0.35	2.5488
0.7	0.5	1.5	0.4	0.7	2	0.5	0.35	2.5487
0.7	0.5	1.5	0.4	0.9	2	0.5	0.35	2.5488
0.7	0.5	1.5	0.4	1.1	2	0.5	0.35	2.5488
0.7	0.5	1.5	0.4	1.1	0.5	0.5	0.35	2.2977
0.7	0.5	1.5	0.4	1.1	2	0.5	0.35	2.5488
0.7	0.5	1.5	0.4	1.1	3.5	0.5	0.35	2.769
0.7	0.5	1.5	0.4	1.1	2	0	0.35	2.5488
0.7	0.5	1.5	0.4	1.1	2	0.5	0.35	2.5488
0.7	0.5	1.5	0.4	1.1	2	0.87	0.35	2.5488
0.7	0.5	1.5	0.4	1.1	2	0.5	0.25	2.5636
0.7	0.5	1.5	0.4	1.1	2	0.5	0.35	2.5488
0.7	0.5	1.5	0.4	1.1	2	0.5	0.5	2.5425

From table 5.3, we observe that;

- i.) An increase in the mass diffusion parameter Sc and removal of suction velocity w_0 causes an increase in the rate of heat transfer Nu
- ii.) An increase in the angle of inclination ψ and modified Grashof number Gc leads to a decrease in the rate of heat transfer Nu
- iii.) An increase in Hall parameter m and Ion-slip parameter n leads to a decrease in heat transfer Nu

iv) A decrease in heat source parameter σ or increase in time t causes an increase in heat transfer

Nu

Table 5.4 Values of skin friction τ_x and τ_y for

$Pr = 0.71, M^2 = 5.0, Gr = -0.4$

n	WO	m	Gc	Sc	$Sigma$	Phi	$Time$	τ_x	τ_y
0	0.5	1.5	0.4	1.1	2	0.5	0.4	-0.00021885	0.00047523
0.5	0.5	1.5	0.4	1.1	2	0.5	0.4	-0.00042832	-0.00035099
1	0.5	1.5	0.4	1.1	2	0.5	0.4	-0.0005871	-0.00026745
0.7	0	1.5	0.4	1.1	2	0.5	0.4	-0.0027	-0.00004362
0.7	0.5	1.5	0.4	1.1	2	0.5	0.4	-0.0004971	-0.0003137
0.7	1	1.5	0.4	1.1	2	0.5	0.4	0.0019	-0.00059513
0.7	0.5	1	0.4	1.1	2	0.5	0.4	-0.00017589	-0.00029941
0.7	0.5	1.5	0.4	1.1	2	0.5	0.4	-0.0004971	-0.0003137
0.7	0.5	2	0.4	1.1	2	0.5	0.4	-0.00071975	-0.0003009
0.7	0.5	1.5	0.4	1.1	2	0.5	0.4	-0.0004971	-0.0003137
0.7	0.5	1.5	1	1.1	2	0.5	0.4	-0.1264	0.01
0.7	0.5	1.5	2	1.1	2	0.5	0.4	-0.336	0.0272
0.7	0.5	1.5	0.4	0.7	2	0.5	0.4	-0.0095	0.0011
0.7	0.5	1.5	0.4	0.9	2	0.5	0.4	-0.0047	0.00033749
0.7	0.5	1.5	0.4	1.1	2	0.5	0.4	-0.0004971	-0.0003137
0.7	0.5	1.5	0.4	1.1	0.5	0.5	0.4	0.0062	-0.0011
0.7	0.5	1.5	0.4	1.1	2	0.5	0.4	-0.0004971	-0.0003137
0.7	0.5	1.5	0.4	1.1	3.5	0.5	0.4	-0.0059	0.00033006
0.7	0.5	1.5	0.4	1.1	2	0	0.4	-0.0014	0
0.7	0.5	1.5	0.4	1.1	2	0.5	0.4	-0.0004971	-0.0003137
0.7	0.5	1.5	0.4	1.1	2	0.9	0.4	0.0026	-0.0014
0.7	0.5	1.5	0.4	1.1	2	0.5	0.3	0.014	-0.00041904
0.7	0.5	1.5	0.4	1.1	2	0.5	0.4	-0.0004971	-0.0003137
0.7	0.5	1.5	0.4	1.1	2	0.5	0.5	-0.0036	0.000081399

From Table 5.4, we observe that;

- i.) An increase in Modified Grashof number Gc and an increase in Hall parameter m leads to a decrease in skin friction τ_x and an increase in skin friction τ_y .
- ii.) An increase in the angle of inclination ψ and Ion-slip parameter n leads to a slight decrease in the skin friction τ_x but an increase in the skin friction τ_y .
- iii.) An increase in the mass diffusion parameter Sc leads to an increase in skin friction τ_x but a decrease in skin friction τ_y .
- iv.) A decrease in heat source parameter σ removal of suction velocity WO and increase in time t cause a decrease in skin friction τ_x and an increase in skin friction τ_y .

Table 5.5 Rate of convection heat transfer Nu , for
 $Pr = 0.71, M^2 = 5.0, Gr = -0.4$

n	WO	m	Gc	Sc	$Sigma$	Phi	$Time$	Nu
0	0.5	1.5	0.4	1.1	2	0.5	0.4	2.5488
0.5	0.5	1.5	0.4	1.1	2	0.5	0.4	2.5488
1	0.5	1.5	0.4	1.1	2	0.5	0.4	2.5488
0.7	0	1.5	0.4	1.1	2	0.5	0.4	2.4073
0.7	0.5	1.5	0.4	1.1	2	0.5	0.4	2.5488
0.7	1	1.5	0.4	1.1	2	0.5	0.4	2.7002
0.7	0.5	1	0.4	1.1	2	0.5	0.4	2.5488
0.7	0.5	1.5	0.4	1.1	2	0.5	0.4	2.5488
0.7	0.5	2	0.4	1.1	2	0.5	0.4	2.5488
0.7	0.5	1.5	0.4	1.1	2	0.5	0.4	2.5488
0.7	0.5	1.5	1	1.1	2	0.5	0.4	2.548
0.7	0.5	1.5	2	1.1	2	0.5	0.4	2.5433
0.7	0.5	1.5	0.4	0.7	2	0.5	0.4	2.5487
0.7	0.5	1.5	0.4	0.9	2	0.5	0.4	2.5488
0.7	0.5	1.5	0.4	1.1	2	0.5	0.4	2.5488
0.7	0.5	1.5	0.4	1.1	0.5	0.5	0.4	2.2977
0.7	0.5	1.5	0.4	1.1	2	0.5	0.4	2.5488
0.7	0.5	1.5	0.4	1.1	3.5	0.5	0.4	2.769
0.7	0.5	1.5	0.4	1.1	2	0	0.4	2.5488
0.7	0.5	1.5	0.4	1.1	2	0.5	0.4	2.5488
0.7	0.5	1.5	0.4	1.1	2	0.9	0.4	2.5488
0.7	0.5	1.5	0.4	1.1	2	0.5	0.3	2.5636
0.7	0.5	1.5	0.4	1.1	2	0.5	0.4	2.5488
0.7	0.5	1.5	0.4	1.1	2	0.5	0.5	2.5425

From table 5.5, we observe that;

- i.) An increase in the modified Grashof number Gc and time t leads to a decrease in rate of heat transfer Nu
- ii.) An increase in the mass diffusion parameter Sc , heat source parameter σ and removal of suction velocity wo leads to an increase in the rate of heat transfer Nu
- iii.) An increase in Hall parameter m , Ion-slip parameter n and angle of inclination ψ has no effect in the rate of heat transfer Nu

VII. CONCLUSION

An analysis of the effects of various parameters on the velocities, temperature and concentration profiles on unsteady, free convection incompressible fluid flow past a semi- infinite vertical porous plate subjected to strong magnetic field inclined at an angle ψ to the plate with hall and ion-slip currents effects has been carried out. In all the considered cases, the applied magnetic field was resolved into two components and our work was restricted to the turbulent boundary layer.

In both cases of $Gr > 0$ and $Gr < 0$ it is observed that a thin boundary layer is formed near the stationary plate. The thickness of these boundary layers increases with increases in either Hall parameter m or ion-slip parameter.

. It was observed that in the absence of mass transfer and cooling or heating of the plate by free convection currents, increases in the Hall parameter m , the mass diffusion Sc , angle of inclination ψ , removal of suction velocity w_0 leads to no effect in temperature. An increase in heat source parameter σ leads to a decrease in primary velocity profiles but to an increase in temperature profiles and secondary velocity profiles. For both $Gr > 0$ and $Gr < 0$ increases in the Hall parameter m , mass diffusion parameter Sc and removal of suction velocity w_0 leads to decrease in primary velocity profiles.

For $Gr > 0$ increases in Hall parameter, angle of inclination, time and modified Grashof number leads to a decrease in secondary velocity profiles. Whereas increase in mass diffusion parameter Sc , heat source parameter and removal of suction velocity leads to an increase in secondary velocity profiles.

For $Gr < 0$ increase in mass diffusion parameter Sc and the removal of suction velocity leads to an increase in secondary velocity profiles but a decrease in primary velocity and concentration profiles. Increase in heat source parameter σ , angle of inclination, time and modified Grashof number Gc leads to an increase in primary velocity profile but a decrease in secondary velocity.

It was observed that an increase in the angle of inclination ψ or ion-slip parameter n causes an increase in primary velocity profiles and a decrease in secondary velocity profiles in both cooling and heating of the plate by free convection currents. Increases in Hall parameter leads to decrease in both primary and secondary velocity profiles. We also observed that increases in time leads to increase in both temperature and concentration profiles, but increase in heat source parameter, angle of inclination and removal of suction velocity causes decrease in temperature profiles.

Further, it is seen that the shear stresses increase due to the primary and secondary flows at the stationary plate with increase in Hall current parameter for fixed value of M^2 , shear stress due to primary velocity τ_x decreases while shear stress due to secondary velocity τ_y increases with increase in ion-slip parameter n .

Increases in modified Grashof number Gc leads to an increase in velocity profiles near the plate but away from the

plate the velocity profiles decrease in the presence of mass transfer and cooling or heating of the plate by free convection currents. It was observed that an increase in the angle of inclination ψ leads to a decrease in both skin friction τ_x due to primary velocity profiles and τ_y due to secondary velocity profiles for $Gr > 0$ and $Gr < 0$. It was observed that increases in Hall parameter m , modified Grashof number Gc , the removal of suction velocity w_0 , or a decrease in heat source parameter σ leads to a decrease in τ_x due to primary velocity profiles and an increase in τ_y due to secondary velocity profiles for $Gr > 0$ and $Gr < 0$. An increase in ion-slip parameter n leads to a decrease in τ_x due to primary velocity profiles and τ_y due to secondary velocity profiles, for $Gr > 0$ but a decrease in τ_x due to primary velocity profiles and an increase in τ_y due to secondary velocity profiles for $Gr < 0$. Finally, increase in the angle of inclination ψ , ion-slip parameter n , Hall parameter m , modified Grashof number Gc and decrease in heat source parameter σ causes a decrease in the rate of convective heat transfer while increase in mass diffusion parameter Sc , time or removal of the suction velocity w_0 leads to an increase in rate of convective heat transfer.

Generally the values of rate of heat transfer Nu for $Gr > 0$ and $Gr < 0$ were found to be approximately the same. This shows that cooling or heating of the plate by free convection currents has no effect on the rate of convection heat transfer at the plate.

We noted that if heat is supplied to the plate at a constant rate, then the flow field is affected. Due to the strong magnetic field, the presence of the hall current affected the flow significantly.

In the presence of hall current cooling of the plate by free convection current increases the thermal boundary layer.

In the power industry, among the methods of generating electric power is one in which electrical energy is extracted directly from a moving conducting fluid. This class of flow has many applications in the design of MHD generators, pumps and flow meters. In many cases the flow in these devices will be accompanied by heat either dissipated internally through viscous heating, joule heating or that produced by electric currents in the walls. We strongly recommend that the designers of these devices should take into consideration the effects of the parameters discussed in this study.

It is hoped that the results will be useful for applications including nuclear engineering especially in designing more efficient cooling system of nuclear reactors and that they can also be used for comparison with other problems dealing with Hall current and ion-slip parameter which might be more complicated. It is also hoped that the results can serve as a compliment to other studies.

VIII. REFERENCES

- [1] Benard K and Moreau R (2008). Magnetohydrodynamic Turbulence at low magnetic Reynolds,” *Annual Review of fluid mechanics*” vol.40, pg.25-45
- [2] Boffetta G , DeLillo , Mazzino A and Vozella L (2012).The ultimate state of thermal convection in Rayleigh- Taylor turbulence, “*Physical D: Nonlinearphenomenon*,” vol.241, pg.137-140
- [3] Bo Lu, Liangwang and Ziaonzhang (2013). Three Dimensional MHD simulation of the electromagnetic flow meter for laminar and turbulent flows. “*International Journal of Fluid flow*,” Vol. 33, 239-243
- [4] Chamkha, J.A, “Unsteady MHD convective heat and mass transfer past a semi-infinite vertical permeable moving plate with heat absorption.” *International Journal of Engineering and Science*, vol.42, pp217-230, (2004)
- [5] Chaundhary R and Shin A. Direct Numerical simulation of transverse and span wise magnetic field effects on turbulent flow a 2:1 aspect ratio. “*International Journal MHD Turbulent fluid flow*,” Vol. 27(2011), pg. 1123-1142.
- [6] Chaundhary R and Shin A. Direct Numerical simulation of transverse and span wise magnetic field effects on turbulent flow a 2:1 aspect ratio. “*International Journal MHD Turbulent fluid flow*,” Vol. 27(2011), pg. 1123-1142.
- [7] Dol, and Hanjalic H.S, (2001). Computational study of turbulent natural convection in aside heated near – cubic enclosure at a high Rayleigh number. “*International. Journal of Heat and Mass Transfer*,” Vol 44, Pg. 2323- 2344.
- [8] Frisch U (1995). Turbulence, Cambridge University Press, “*Plasma and Fluid Turbulence*,”
- [9] Hatton Y, Toshihiro T, Ysutaka N and Nabukazo T (2006). Turbulence characteristics of natural convection boundary layer in air along a vertical plate heated at high temperatures,” *International Journal of heat and fluid flow*,” vol.27, pg. 445-455
- [10] Kenjeres J, Gunarjo S, and Hanjalic K (2004).Contribution to elliptic relaxation modeling of turbulent natural and mixed convection, in: *International Symposium*. Advanced.
- [11] Kinyanjui M, Emmah M., Marigi J and Kwanza K (2012). Hydromagnetic turbulent flow of a rotating system past a semi-infinite vertical plate with hall current. “*International Journal of Heat and Mass transfer*,” Vol.79, pg. 97-119.
- [12] Kinyanjui and Uppal, M, and Uppal, S.M, “MHD stokes problem for a vertical infinite plate in a dissipative rotating fluid with hall current” , *Journal of Magneto hydrodynamics and plasma Research*, Vol. 8 No. 1, pp 15-30,(1998)
- [13] Kitagawa A. and Murai Y (2013). Natural convection heat transfer from a vertical heated plate in water with micro bubble injection,” *Chemical Engineering Science*,”vol.99, pg.215-224
- [14] Mohamed O and Nicolas G (2006). Numerical Analysis of turbulent buoyant flows in enclosures: influence of grid and boundary conditions.
- [15] Nakaharai H and Yokomine J (2007). Influence of a transverse magnetic field on the local and average heat transfer of an electrically conducting fluid.” *International Journal of Heat and Mass transfer*,” Vol. 32 , pg. 23-28
- [16] Rodriguez-Sevillano (2012). On the onset of turbulence in natural convection on inclined plates, “*Experimental Thermal and fluid Science*,” Vol.35, pg.68-72
- [17] Sanvicentre E, Giroux- Julien S, Menez C and Bouia H (2013). Transitional natural convection flow and heat transfer in an open channel, “*International Journal ofThermal Sciences*,” vol.99,pg. 215-224
- [18] Satale S, Kunug T, Takase K and Ose Y (2006). Direct numerical simulation of turbulent flow under a uniform magnetic field for large-scale structures at high Reynolds number. “*Physical Fluids*” vol. 18, pg. 125-106
- [19] Shin- ichi S, Chikamasa C, Kazuyuki M and Kunugi T (2010). Direct Numerical Simulation of unstable stratified turbulent flow under a magnetic field. “*International Journal of Heat and fluid flow*,” Vol.85, pg. 1326-1330
- [20] Soundalgekar,V.M, Bhat,J.P, and Mohiuddin, M. “finite difference analysis of free convection effects on stokes problem for a vertical plate in a dissipative fluid with constant heat flux”. *International Journal of Engineering and Science*, vol. 17, No. 12, pp 1283-1288,(1979).
- [21] Xenos M, Trirtzilaki E and Kafoussiass N (2009). Optimizing separation of compressible boundary-layer flow over a wedge with heat and mass transfer. “*International Journal of Heat and Mass transfer*,” Vol. 52, pg. 488-496.
- [22] Yamamoto Y (2008) DNS and k- \mathcal{E} model simulation of MHD turbulent channel flow with heat transfer,” *International Journal of heat and mass transfer*,” Vol. 28, pg.1-13
- [23] Yoshinobu Y and Tomoaki T (2011). Heat transfer degradation in high Prandtl number fluid. “*International Journal of Heat and fluid flow*,” Vol.22, pg. 67-83.
- [24] Zoynal M, Abedin M, Toshihiro T and Jinho L (2012). Turbulence characteristics and vertical structures in combined- convection boundary layers along a heated vertical flat plate, “*International Journal of heat and masstransfer*,” vol.55, pg.3995-400